Journal of Applied Sciences

ISSN 1812-5654

science alert

ANSInet
an open access publisher
http://ansinet.com

Journal of Applied Sciences 8 (24): 4472-4486, 2008
ISSN 1812-5654

Applying Discriminant Analysis to Separate the Alteration Zones Within the Sungun Porphyry Copper Deposit

Omid Asghari and Ardeshir Hezarkhani
Department of Mining and Metallurgy, Amirkabir University of Technology,
424 Hafez Ave., Tehran, Iran

Abstract: This research tries to separate the potassic and phyllic alteration zones in the Sungun porphyry copper deposit based on fluid inclusion data through applying discriminant analysis. The Sungun porphyries occur as stocks and dikes ranging in composition from quartz monzodiorite through quartz monzonite. Four types of hypogene alteration are developed at Sungun: potassic, phyllic, propylitic and argillic. Based upon their phase content, three types of fluid inclusions are typically observed at Sungun: (1) vapor-rich, two-phase, (2) liquid-rich two-phase and (3) multi-phase. Halite is the principal solid phase in the latter. The primary multiphase inclusions within the quartz crystals in quartz-sulfide and quartz-molybdenite veinlets (quartz associated with sulfide minerals) were chosen for micro-thermometric analysis and considered to calculate the geological pressure and hydrothermal fluid density. Discriminant analysis is a multivariate statistical method which can be applied to separate the alteration zones e.g., based on the fluid inclusions data. Six variables have been measured and calculated for each separated sample, including the homogenization temperature, salinity, pressure, depth, density and the Cu grade. To find the linear combination of these variables which produces the maximum difference between the defined alterations, we defined a function that produced a significant difference, a critical score ($R_0 = 1.83$), as the separation boundary. It is expected that the values larger than R_0 belong to potassic alteration and less than R_0 belong to phyllic alteration. By using this function we can allocate the new fluid inclusions with unknown alteration to one of the two original alteration of potassic or phyllic on the basis of the linear discriminant function of their variables.

Key words: Fluid inclusion, porphyry copper deposit, discriminant analysis, alteration

INTRODUCTION

Porphyry Copper deposits generate where magmatic-hydrothermal fluids are expelled from a crystallizing magma (Rapien *et al*., 2003). Cooling, depressurization and reaction between the fluids and the wall rocks cause metals to precipitate in and around the fractures, forming veins with alteration envelopes. Alteration assemblages and associated mineralization in porphyry ore deposits develop from huge hydrothermal systems dominated by magmatic and meteoric fluids (Sillitoe, 1997; Watanabe and Hedenquist, 2001; Meinert *et al*., 2003). These systems develop in and adjacent to subvolcanic porphyritic intrusions that are apophyses to deeper-seated magma bodies (Sillitoe and Hedenquist, 2003; Heinrich *et al*., 2003).

Fluid inclusions analysis indicate that they are trapped in porphyry Cu deposits typically include halite-saturated brines and low-salinity vapor inclusions (Heinrich, 2005). The formation of brine and vapor is inferred to result from a miscibility gap in the $NaCl-H_2O$ system that coincides with the pressure (< 2200 bars) and temperature (300 to 600°C) where most porphyry Cu deposits form (Kehayov *et al*., 2003).

Fluid inclusion studies in Porphyry Copper Deposits (PCDs) have proven to be an important tool to constrain the physico-chemical conditions of the hydrothermal fluids responsible for vast and pervasive alteration and mineralization processes. These fluid inclusion studies have shown many common features in such deposits throughout the world (Ulrich *et al*., 2001; Redmond *et al*., 2004).

At Sungun deposit, numerous cross-cutting quartz veinlets and micro-veinlets, developed in various stages of alteration and mineralization, provided suitable material for fluid inclusions investigations. Based upon systematic sub-surface sampling, more detailed studies of fluid inclusions were carried out by Calagari (2004) and comprehensive micro thermometric data were accumulated. Additional fluid inclusion study on the Sungun PCD was presented by Hezarkhani and Williams-Jones (1998).

Corresponding Author: Omid Asghari, Department of Mining and Metallurgy, Amirkabir University of Technology, 424 Hafez Ave., Tehran, Iran Tel: 009821-64542949 Fax: 009821-66405846

In a porphyric system such as sungun, the hydrothermal fluid can cause different alterations assemblages based on the temperature, pressure, salinity and other related conditions. These parameters can control precipitation of minerals with different stabilities (Hezarkhani *et al*., 1999). Generally, we can determine the alteration type using the microscopic studies of the minerals and instrumental analysis. In this study, however, we have tried to indirectly investigate (beside the microscopic studies) the alteration assemblage based on fluid inclusion study and achieved parameters: homogenization temperature, salinity, density and pressure of hydrothermal fluid and two other auxiliary parameters: containing copper and z (elevation level). The innovation of this study is the use of discriminate analysis, a multivariate statistics method, for quantitatively separation and intensity determination of the alterations. This method decreases the multi-dimensional space including several parameters into a one-dimension, in a way the maximum separation could be observed in this axis. It is closely related to multiple regression and trend-surface analysis (Davis, 2002).

GEOLOGICAL SETTING

The Sungun PCD is located in about 100 km NE of Tabriz, in the NW part of Iran. The Sungun porphyries intruded, Upper Cretaceous carbonate rocks, a series of Eocene arenaceous-argillaceous rocks and a series of Oligocene dacitic breccias, tuffs and trachy-andesitic

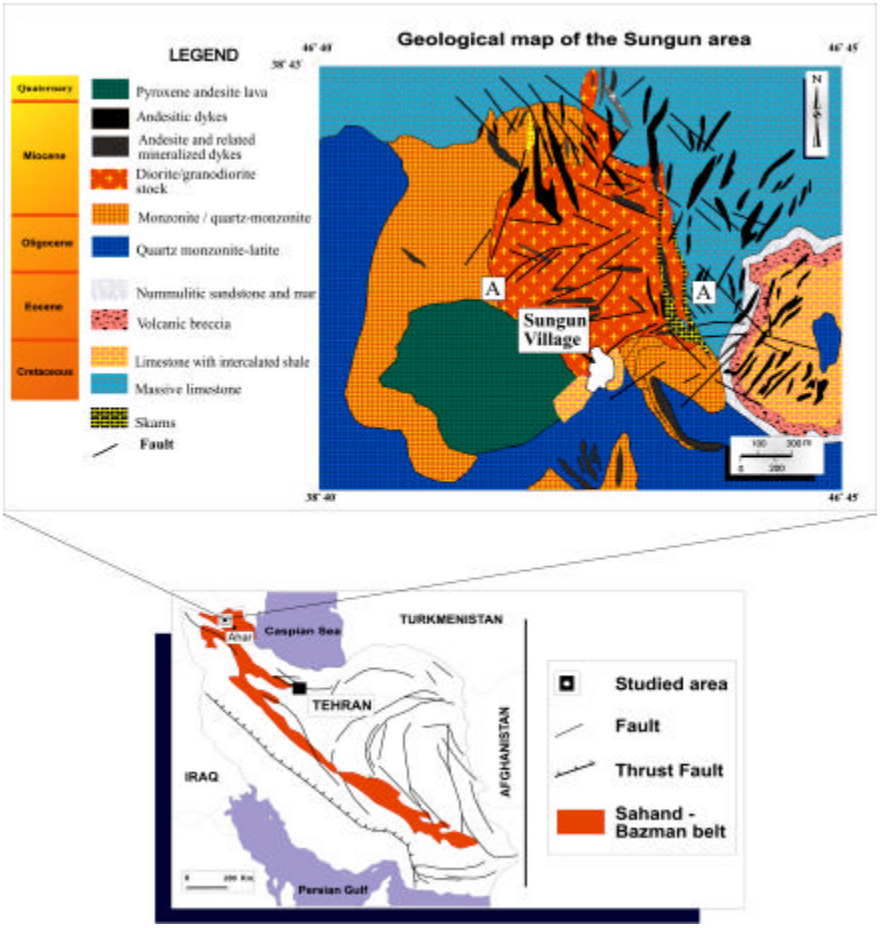

Fig. 1: Geological map of Iran (Stocklin and Stocklin, 1977; Shahabpour and Doorandish, 2007) showing Sahand-Bazman belt: Calc-alkaline volcanic and Quartz monzonite and quartz diorite intrusions of dominantly Miocene age, hosting Cu-Mo porphyry style mineralization and geological map of the Sungun deposit area, showing field relationships among the various subtypes of Sungun intrusive rocks and the outline of the mineralized zone. The porphyritic quartz monzonite rims all other porphyritic plutons to the South and West and Cretaceous limestone and associated skarn border the North and East

lavas (Hezarkhani and William-Jones, 1998, 2006). The Sungun porphyries, which contain >500 Mt of sulfide reserves grading 0.76% Cu and ~0.01% Mo, occur as stocks and dikes and are a series of calc-alkaline igneous rocks with a typical porphyritic texture (Hezarkhani and Williams-Jones, 1998). They are situated in the northwestern part of a NW-SE trending Cenozoic magmatic belt (Sahand-Bazman) within which the Sarcheshmeh PCD is also located. The Sar Cheshmeh porphyry copper mine is located in the Central Iranian Volcanic Belt (CIVB), in Kerman Province of Iran. The deposit contains 1200 million tons ore of 0.69% Cu and 0.03% Mo (Shahabpour and Doorandish, 2007) (Fig. 1). The Sungun stocks are divided into two groups: Porphyry Stocks I is typically quartz monzodiorite. Porphyry Stock II (which is investigated in this research) hosts the Sungun PCD and varies in composition from quartz monzonite through granodiorite to granite.

HYDROTHERMAL ALTERATION AND MINERALIZATION

Alteration assemblages and related mineralization in the Sungun porphyry copper deposit have been investigated by geological mapping (Fig. 2) and detailed studies of the mineralogy, petrography and chemistry of a large number of drill cores and outcrop samples from various parts of the stock (Fig. 3). Hydrothermal alteration and mineralization at Sungun are centered on the stock and were broadly synchronous with its emplacement. Early hydrothermal alteration was dominantly potassic and propylitic and was followed by later phyllic and argillic alteration.

Potassic alteration: The earliest alteration is represented by potassic mineral assemblages developed pervasively and as halos around veins in the deep and central parts of the Sungun stock (Hezarkhani and Williams-Jones, 1998). Potassic alteration is characterized by K feldspar. They also mentioned that this alteration displays a close spatial association with mineralization; perhaps as much as 60% of the copper and all the molybdenum were emplaced during this alteration episode (Hezarkhani and Williams-Jones, 1998). On average, potassically altered rocks contain 28% plagioclase, 33% orthoclase, 20% quartz, 15% ferromagnesian minerals (mainly biotite and sericite and chlorite after biotite) and 4% chalcopyrite, pyrite, zircon, scheelite, uraninite, bismuthinite and rutile (Hezarkhani, 2006b) (Fig. 2).

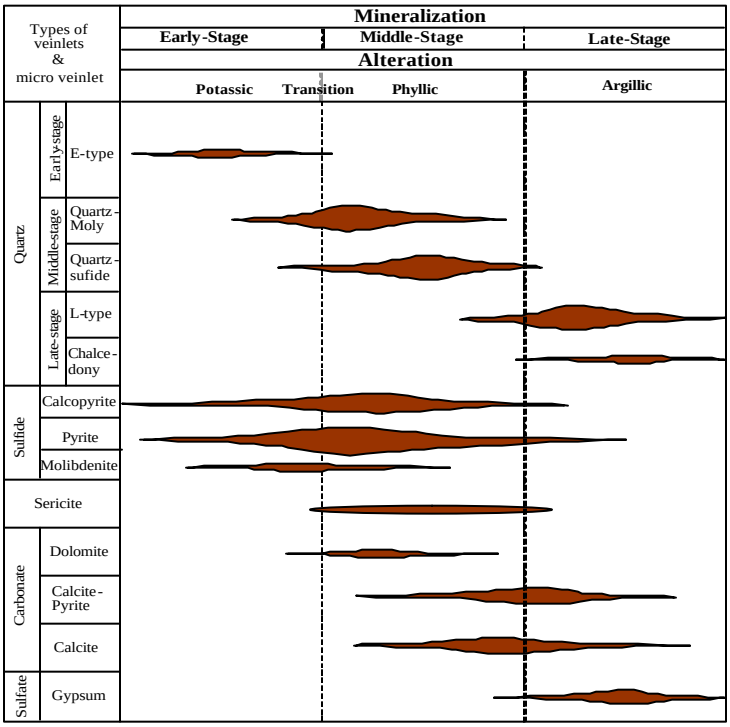

Fig. 2: Paragenetic sequence of the development of various types of veinlets and micro-veinlets in porphyry stock II at Sungun. The thickness of the horizontal bars is related to the relative abundance of the veinlets in the porphyry system (Hezarkhani and Williams-Jones, 1998; Calagari, 2004)

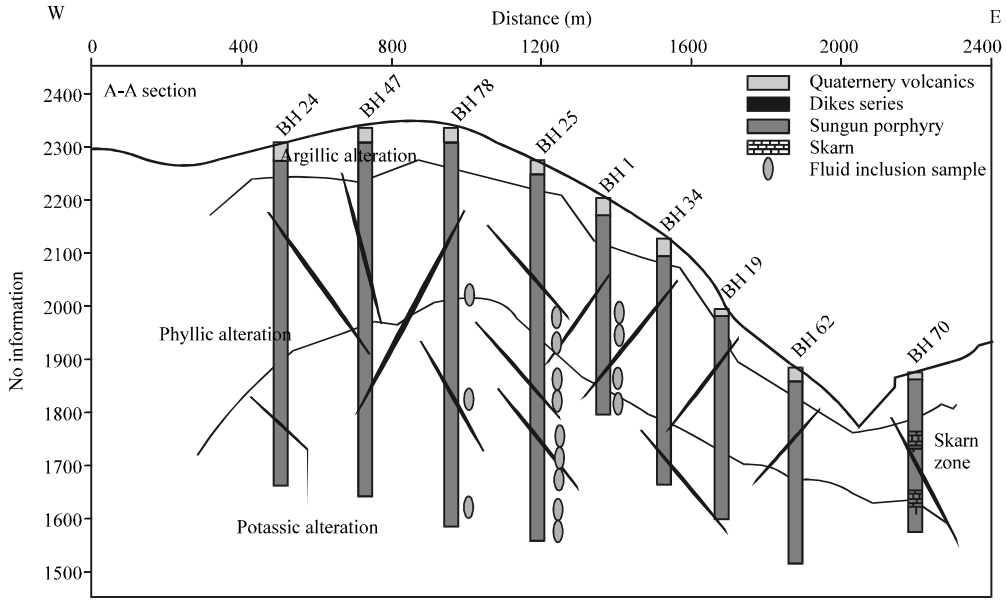

Fig. 3: Profile along A-A in Fig. 1 showing the position of diamond drill holes, dike series and the pattern of hypogene alteration zones (potassic, phyllic and argillic) in porphyry stock II

Phyllic alteration: The change from transition alteration to phyllic alteration is gradual and is marked by an increase in the proportion of muscovite. Phyllic alteration is characterized by the replacement of almost all rock-forming silicates by sericite and quartz and overprints the earlier formed potassic and transition zones. Pyrite forms up to 5 vol. percent of the rock and occurs in veins and disseminations. Quartz veins are surrounded by weak sericitic halos (Fig. 2). Vein-hosted pyrite is partially replaced by chalcopyrite. Silicification was synchronous with phyllic alteration and variably affected much of the stock and most dikes. This observation is supported by whole-rock chemical analysis, which show that Si was added in higher than for any other stage of the alteration (Hezarkhani and Williams-Jones, 1998). In contrast to the transition zone, appreciable Cu was added to the rock during phyllic alteration. It is difficult to separate transition and phyllic alteration because of intense silicification during the latter alteration (Fig. 3).

Mineralization: Hypogene copper mineralization was introduced during potassic alteration and to a lesser extent during phyllic alteration and exists as disseminations and in veinlet form. During potassic alteration, the copper mineralization consisted of chalcopyrite and minor bornite; later hypogene copper mineralization consisted mainly of chalcopyrite (Fig. 2). Hypogene molybdenum mineralization (molybdenite) was concentrated mainly in the deep part of the stock and is associated exclusively with potassic alteration, where it is found in quartz veins accompanied by K-feldspar, anhydrite, sericite and lesser chalcopyrite. Alteration of feldspars and biotite (from potassically altered rocks) was accompanied by an increase in sulphide content outward from the central part of the stock. Copper mineralization increases toward the margins of the central potassic zone, from less than 0.20 to 0.85 wt.%. There is also a positive correlation between silicification and copper mineralization. The maximum Cu grade is associated with biotite, orthoclase and sericite (potassic zone) while the pyrite content is highest (3-10 vol.% of the rock) in the marginal quartz-sericite (phyllic) zone. The ratio of pyrite to chalcopyrite in the zone of richest hypogene copper mineralization in the potassic alteration zone is as low as 4:1, but toward the margins of the stock the ratio increases to 15:1.

FLUID INCLUSIONS PETROGRAPHY

The Sungun deposit contains well-developed stockwork mineralization that is concentrated in the potassic and transition zones (the transition zone is actually the outermost part of the potassic zone and is characterized by a low content of biotite and abundant sericitization). Based on mineralogy and cross-cutting relationships, it is possible to distinguish four main groups of veins representing four episodes of vein formation: (I) quartz+molybdenite+anhydrite±K-feldspar

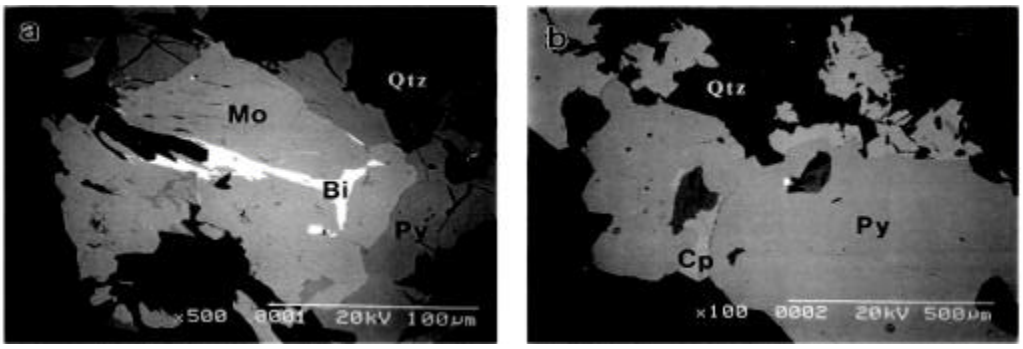

Fig. 4: Scanning electron photomicrographs, (a) Molybdenite with associated anhedral bismuthinite and pyrite and (b) Quartz associated with pyrite altered to chalcopyrite; Bi: Bismuthinite, Cp: Chalcopyrite, Mo: Molybdenite, Py: Pyrite, Qtz: Quartz

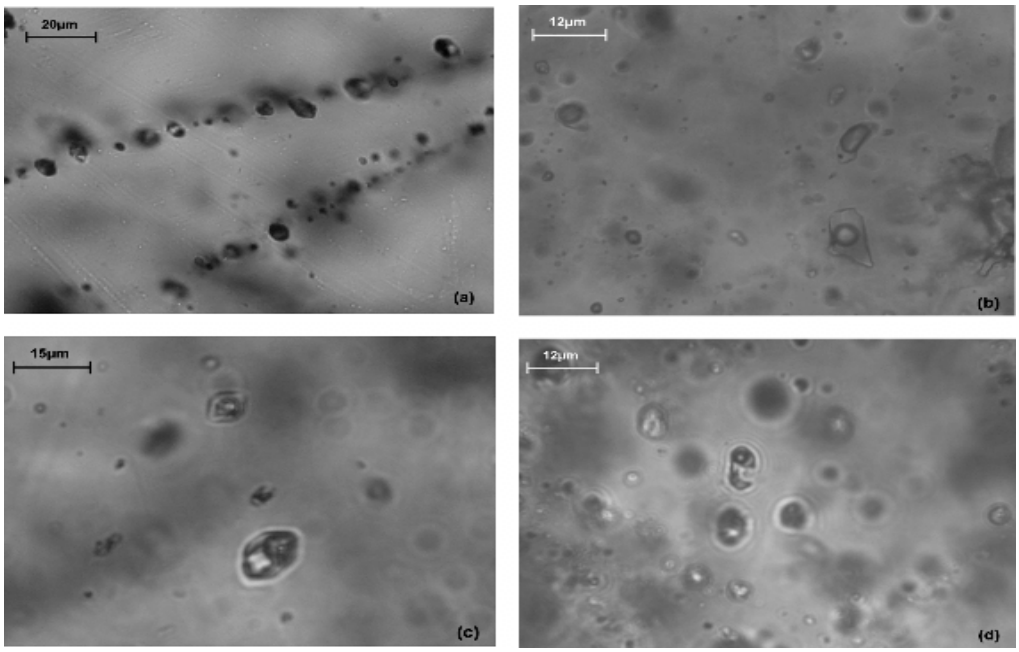

Fig. 5: Photomicrographs of different inclusion types within mineralized quartz vein from Sungun. (a) Secondary fluid inclusions; (b) Secondary biphase (VL and LV) inclusions, (c) Primary polyphase inclusion from potassic alteration assemblage (sample No. 42) and (d) Primary inclusion from Phyllic alteration assemblage (sample No. 18). All photographs were taken at ambient laboratory temperature

with sporadic pyrite, chalcopyrite and bornite, (II) quartz +chalcopyrite+pyrite±molybdenite, (III) quartz+pyrite+ calcite±chalcopyrite+anhydrite (gypsum)+molybdenite and (IV) quartz and/or calcite and/or gypsum ± pyrite.

Fluid inclusions are abundant in quartz of all vein types and range in diameter from 1 µm up to 15 µm. The majority of inclusions examined during this study had diameters of 4-12 µm. They are also common in quartz, but are too small (<3 µm) to be analyzed microthermometrically. Only fluid inclusions within the quartz crystals in quartz-sulfide and quartz-molybdenite veinlets were chosen for micro-thermometric analysis for two important reasons: (1) the inclusions are intimately associated with copper and molybdenum sulfides (Fig. 4a, b), (2) these veinlets contain inclusions >7 µm which allows for more confident thermometric analysis. The individual quartz crystals contain numerous cross-cutting micro-fractures along which fluid inclusions are aligned (Fig. 5a). A preliminary classification of fluid inclusions was carried out based on the number, nature and relative

proportions of phases at room temperature and led to recognition of the following types of fluid inclusions:

LV inclusions consist of liquid+vapor±solid phases with the liquid phase volumetrically dominant. These fluid inclusions are common in all mineralized quartz veins and are abundant in group 2 and 3 veins (Fig. 5b). The diameters of these fluid inclusions ranges from 3 to 12 μm. LV inclusions are found in all vein groups, but occur in variable proportions. They are most abundant in the group 2 and 3 veins and rare in group 1 veins. Most LV inclusions are distributed along healed fractures and are of secondary origin.

VL inclusions are found in quartz phenocrysts from fresh rocks and in group 1, 2 and 3 quartz veins. Some of these inclusions occur in growth zones in group 1 and 2 quartz veins, where they are accompanied by LVH fluid inclusions, indicating that most of them are primary. VL inclusions are generally elongated and have rounded ends, but some have negative crystal shapes. Some of the VL inclusions have variable liquid-vapor ratios and may have formed from the necking down of LVH inclusions or heterogeneous entrapment of liquid and vapor.

LVH inclusions are found in all veins, from the deepest, potassically altered part of the stock through to the shallow level veins (Fig. 5b, c). The fluids occupy cavities ranging from 1 to 15 μm in diameter. The coexistence of LVH inclusions and vapor-rich inclusions with consistent phase ratios in the growth zones of quartz grains from potassic and phyllic alteration zones suggests a primary origin and coexistence of two immiscible aqueous fluids. The majority of LVH inclusions examined during this study had diameters of 4-12 μm. Fifty seven sub-surface samples containing quartz veinlets from diamond drill holes within the hypogene alteration zones in porphyry stock II were selected for thermometric analysis.

FLUID INCLUSION INVESTIGATIONS

The samples were initially prepared for microscopic examination. Based on mineral content, we found the origin of alteration and categorized them into potassic and phyllic. The distribution pattern, shape, size and phase content of fluid inclusions within the quartz crystals were examined applying a microscope (Table 1). Temperatures of phase changes in fluid inclusions were measured with a Fluid Inc. USGS-type gas-flow (Linkam Operating System) stage, which operates by passing preheated or precooled N_2 gas around the sample. Stage calibration was performed using synthetic and/or well-known fluid inclusions. Accuracy at the standard reference temperatures was ±0.2 at -56.6°C (triple point of CO_2), ±0.1°C at 0°C (melting point of ice), ±2°C at 374.1°C (critical homogenization of H_2O) and ±9°C at 573°C (alpha to beta quartz transition). The heating rate was approximately 1°C/min near the temperatures of phase transitions.

Table 1: Statistical parameters of raw data based on fluid inclusion study and micro thermometry for 845 measurements in 57 samples

Statistical parameter	Salinity (%)	T_H (°C)	T_m (°C)	T_e (°C)	Size (μ^2)	L/V ratio
Mean	23.9	355	-7.5	-38.0	22.4	2.9
SD	18.7	93	5.5	11.7	10.4	2.7
SV	348.0	8586	30.3	138.0	109.0	7.1
Minimum	0.2	88	-33.0	-67.0	6.0	0.1
Maximum	65.5	620	-0.5	-4.0	70.0	19.0

SD: Standard Deviation, SV: Sample Variance

Quartz crystals exist within almost all types of quartz veinlets (late-type, quartz-sulfide, quartz-molybdenite and early type (Fig. 2). Based upon their phase content, three types of inclusion are present at Sungun: (1) vapor-rich 2-phase, (2) liquid-rich 2-phase and (3) multi-phase solid. Halite crystals are larger than the other solids and can be readily distinguished by their cubic shape. Similar characteristics are seen in fluid inclusion assemblages from other PCDs.

Micro-thermometric analysis: Thermometric analysis were performed principally on fluid inclusions which were relatively large (>7 μm). Freezing and heating experiment helped determine the approximate salinity (wt.% NaCl equivalent) and homogenization temperature (T_H), respectively (Table 1). The heating stage was used for all types of inclusion. For non-halite bearing inclusions the homogenization temperature of liquid and vapor (either L+V→L or L+V→V) was recorded. In the halite-bearing inclusions, two points: (1) $T_{s(NaCl)}$ (the temperature at which halite dissolves) and (2) $T_{H(L-V)}$ (temperature of vapor and liquid homogenization) were recorded.

Homogenization temperatures: The temperatures of initial (T_e) and final melting of ice ($T_{m\,ice}$) were measured on types LV, VL and LVH fluid inclusions. The temperature of initial ice melting (T_e) of most LV fluid inclusions was between -23 and -24°C, suggesting that NaCl is the principal salts in solution. The T_e value of VL fluid inclusions ranges from -20 to -46°C with a mode of ~-22°C, suggesting that Na and K are the dominant cations in the solution, but there may be another component for example Mg and Ca which could not be measurable by this method. The low Te (-31 to -46°C) for some of the VL inclusions could indicate that these inclusions are the product of necking down of LVH inclusions. The eutectic temperatures that could be measured in LVH inclusions range from 30 to -64°C, suggesting important concentrations of Fe, Mg, Ca and/or other components in addition to Na and K in this

type of inclusion. The T_{mice} values for LV inclusions range from -5 to -8°C, corresponding to salinities of 5.7 wt.% NaCl equivalent, respectively (Sterner *et al*., 1988). The T_{mice} value for VL inclusions varies from -0.4 to -12°C, which corresponds to a salinity of between 0.8 and 12.2 wt.% NaCl equivalent.

LV fluid inclusions homogenize to liquid T_h(L+V→L) at temperatures between 523 and 298°C. Most of VL inclusions homogenize to vapor T_h(V+L→V) between 351° and 600 (°C). The frequency distribution of halite-bearing inclusions homogenizing by halite disappearance ($T_{s(NaCl)} > T_{H(L-V)}$) display a wide range of $T_{s(NaCl)}$ values, varying from 220 to 583 (°C). Salinities based on the halite dissolution temperature range from 29.7 to 61.1 wt.% NaCl equivalent (Sterner *et al*., 1988). The halite-bearing inclusions homogenizing by simultaneous disappearance of halite vapor and/or by vapor disappearance ($T_{s(NaCl)} = T_{H(L-V)}$) show a similar range of distribution and their $T_{H(L-V)}$ values vary from 200 to 580°C. Some LVH inclusions homogenized by vapor disappearance and by contrast, some LVH inclusions homogenized mainly by halite dissolution. Anhydrite and chalcopyrite did not dissolve on heating to temperatures in excess of 600°C. Chalcopyrite was identified on the basis of its optical characteristics (opacity and triangular cross section) and composition in opened inclusions (SEM-EDAX analysis yielded peaks for Cu, Fe and S). Anhydrite forms transparent anisotropic prisms and was shown by SEM-EDAX analysis to consist only of Ca and S (elements lighter than F could not be analyzed) (Hezarkhani and Williams-Jones, 1998).

Salinity in the inclusion fluids: Halite-bearing and non-halite-bearing liquid-rich inclusions at Sungun exhibit a wide variation in salinity, ranging from 0.2 to 65.5 wt.% (Fig. 6).

As shown by Fig. 7a, it can sharply divide into 2 population. Low salinity (less than 27 wt.% NaCl) and high salinity (between 27 wt.% NaCl and 65.5 wt%). In high salinity fluid inclusions (Fig. 7b), there is a good correlation between the salinity and their homogenization temperature and the correlation coefficient is around 84%

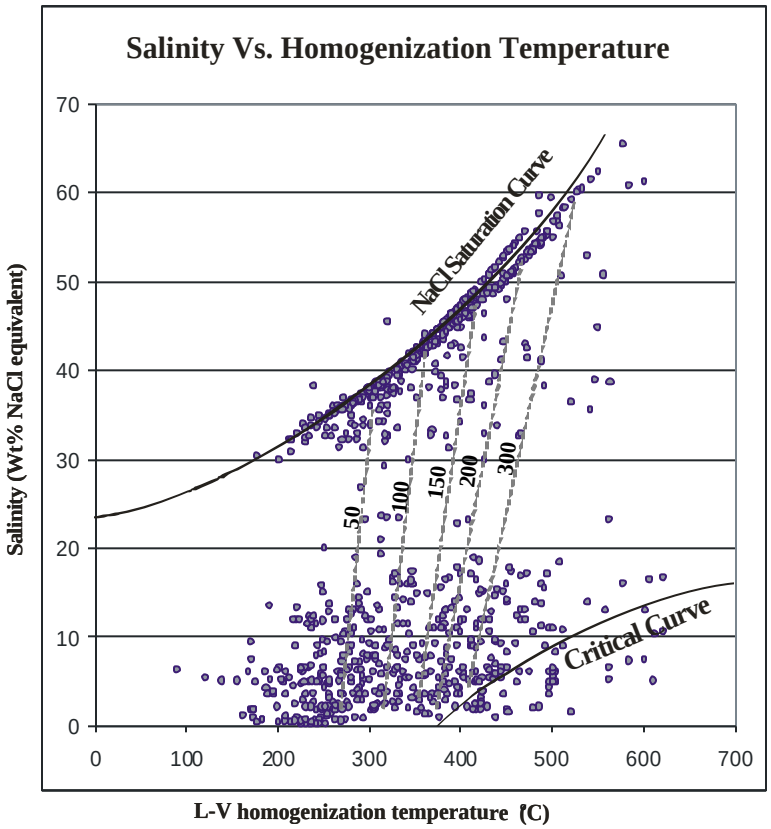

Fig. 6: Salinity versus $T_{H(L-V)}$ showing the distribution pattern of the data points relative to the NaCl saturation and critical curves. Dashed lines referring to vapor pressures of NaCl solutions at the indicated temperatures and salinity

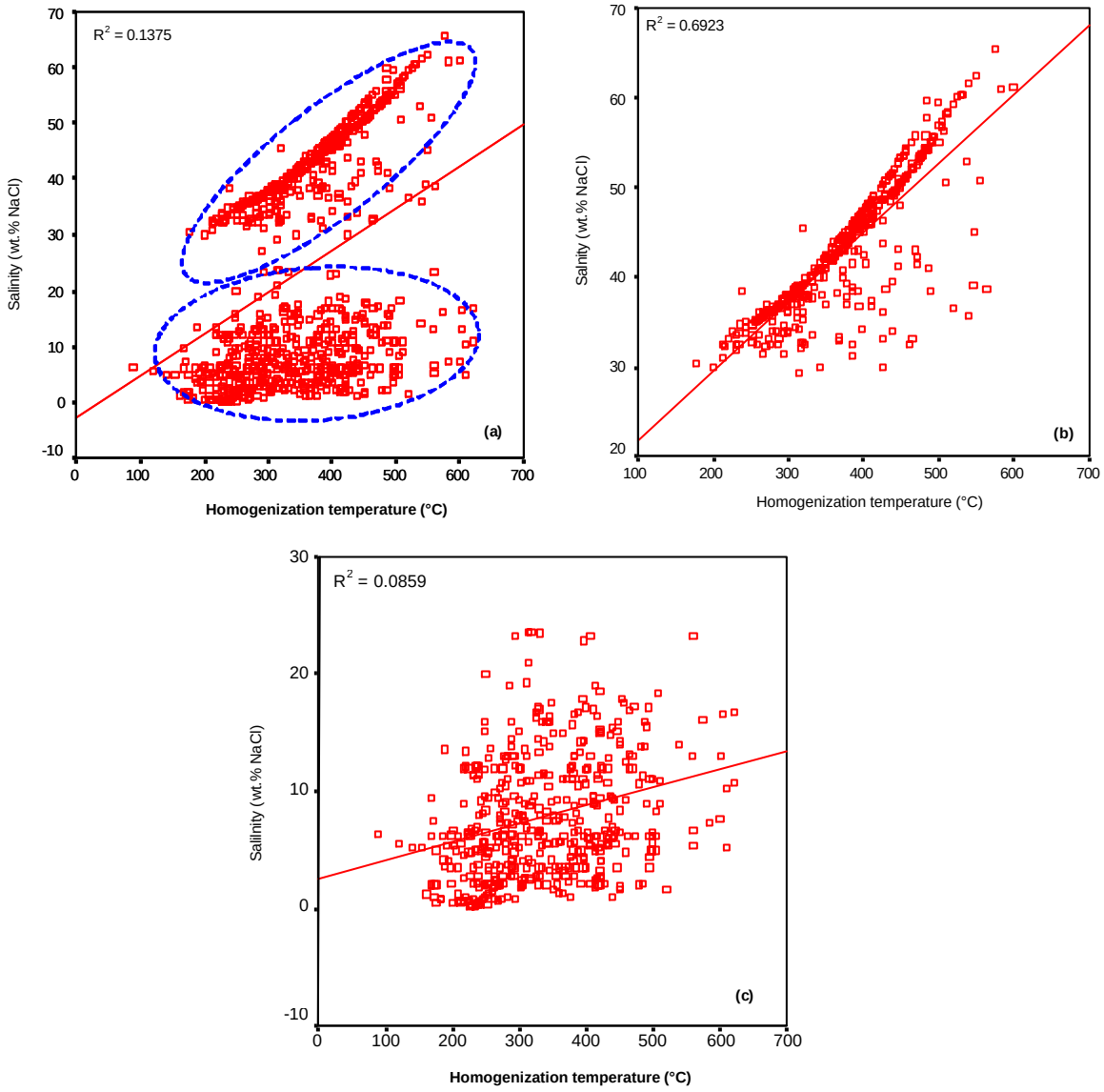

Fig. 7: (a) Scatter plot of salinity vs. homogenization temperature showing two different behaviors in salinity and Th, (b) a relatively high coherence between high salinities and Th (R^2 = 0.6923, coherent coefficient = 0.83) and (c) a low coherence between low salinities and Th (R^2 = 0.0859, coherent coefficient = 0.29)

(R^2 = 0.69). In low salinity fluid inclusions (Fig. 7c), the salinity and the homogenization temperature does not show any harmonic relationships (R^2 = 0.09). There are many halite-bearing fluid inclusions which have $T_{s(NaCl)} > T_{H(L-V)}$ and the discrepancy between $T_{s(NaCl)}$ and $T_{H(L-V)}$ in some inclusions may reach ~98°C (Fig. 8). These inclusions may suggest entrapment of supersaturated (with respect to NaCl) fluid or high pressure conditions of entrapment. However, there are still many halite-bearing inclusions whose data points lie around and below the halite saturation curve ($T_{s(NaCl)} < T_{H(L-V)}$) (Fig. 4) which, in turn, denotes trapping of saturated and under saturated fluids, respectively.

Based on the Brown and Lamb (1989) method, to measure the geological pressure, the applied fluid inclusions must be halite- and gas-bearing with high salinity ones, which is why that these type of fluid inclusions are used from now on. Table 2 shows the statistical properties of the fluid inclusions with the salinities more than 27 wt.% equivalent.

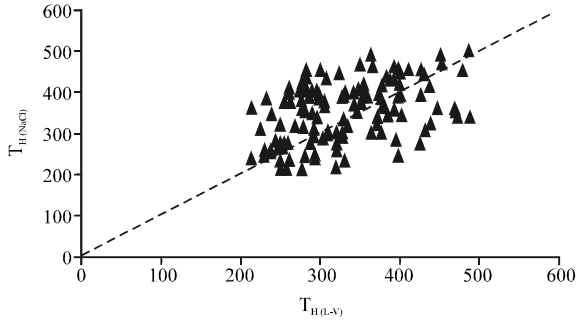

Fig. 8: Liquid-vapor homogenization temperature [$T_{H(L-V)}$] versus halite dissolution temperature [$T_{H(NaCl)}$] for halite - bearing inclusions at Sungun (the diagonal line [$T_{H(L-V)} = T_{s(NaCl)}$] from Shepherd *et al.* (1985)). For calculating the pressure we used points over the diagonal line, where, $T_{s(NaCl)} > T_{H(L-V)}$

Table 2: Descriptive statistics of row data for high salinity inclusions (more than 27 wt.% NaCl)

Statistical parameter	Salinity (%)	T_H (°C)	T_m (°C)	T_e (°C)	Size (μ^2)	L/V ratio
Mean	43.0	375	-11.6	-46.9	24.5	3.4
SD	7.6	82	6.4	9.1	12.4	2.1
SV	57.0	6664	40.3	82.5	154.0	4.3
Minimum	29.0	176	-33.0	-67.4	8.0	0.3
Maximum	65.5	600	-1.2	-26.0	70.0	9.0

OTHER VARIABLES

The point pressure and hydrothermal fluid density in the NaCl-H_2O system is calculated for 47 samples with using 3 parameters including Th→Halite (°C), Th→Vapor (°C) and salinity (wt.% NaCl), based on Brown and Lamb (1989) equation by the Flincor software (Brown, 1989). Fluid pressures varies from 261 to 2148 bars (Table 3). The thirteen diamond drill holes within the Porphyry Stock II are drilled and 57 samples from drilled holes are collected. Approximately 10-20 g of each sample location from drilled cores (from quartz veins associated with ore minerals, where fluid inclusion chips have been prepared) were crushed and powdered for XRF analysis. The XRF analysis were carried out and accuracy and precision of the analytical procedure has been checked and the Cu grade of each sample determined.

All samples have locations which are identified with x_i, y_i, z_i. So, each sample has its own elevation. Regarding to the geometric models of porphyry copper deposits, the potassic alteration zones are located in core and phyllic zones lie in shallower part of the system, therefore it is assumed that the elevation of each sample could be considered as a parameter for alteration separation. As shown in Fig. 9 there is not a high coherency between the sample elevations and the other variables, so it's a very important note to consider all variables, independent from the sample elevation (Tabachnick and Fidell, 2000).

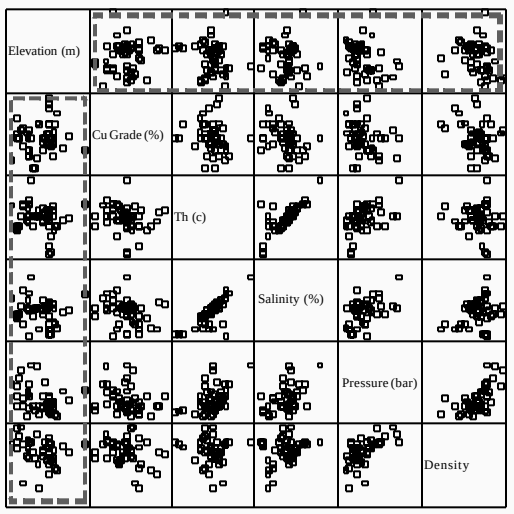

Fig. 9: Matrix scatter plot of 6 measured and calculated parameters like; samples elevations from sea level (m), Cu grade (%), Homogenization temperature, Salinity (NaCl wt.% equiv.), Pressure (bar) and hydrothermal fluid density. This chart indicates that it is possible to identify all variables, independent from the elevation since there is not a high coherency between their values

Table 3: Descriptive statistics of 25 samples from phyllic alteration and 22 samples from potassic alteration

Alteration	1	2	3	4	5	6	7	8
Potassic	Mean	1695	0.57	414	46.3	368	1195	1.120
	SD	116	0.27	56	5.7	63	498	0.040
	Var.	13351	0.07	3181	32.7	3925	247652	0.002
	Min.	1543	0.10	337	32.6	277	303	0.980
	Max.	2080	1.31	583	60.9	550	2148	1.190
Phyllic	Mean	1811	0.68	376	42.5	354	623	1.080
	SD	71	0.25	64	5.8	66	222	0.040
	Var.	5092	0.06	4039	34.0	4374	49497	0.002
	Min.	1622	0.12	220	33.0	200	261	0.970
	Max.	1959	1.21	460	54.6	451	1214	1.150
Total	Mean	1757	0.63	394	44.2	360.	891	1.100

(1) Descriptive, (2) Elevation, (3) Cu, (4)Th→H, (5), Salinity, (6)Th→V,(7) Pressure and (8) Density

As discussed earlier, the analysis were done on the three-phase fluid inclusions that were in the quartz veins adjacent to the mineralization (in different alterations). As we expected, this fluid inclusions shows high salinity. With the investigation of the Table 3, it could be seen that the average salinity in potassic alteration is a little bit higher than the average salinity of the phyllic alteration, but they are very close to each other, as mentioned by Hezarkhani and Williams-Jones (1998).

DISCRIMINANT ANALYSIS THEORY

The discriminant function analysis involves identification or the placing of objects into predefined groups (Davis, 2002). This method consists of finding a transform which gives the maximum ratio of the difference between two group multivariate means to the multivariate variance within the two groups (McLachlan, 1992). It is closely related to multiple regression and trend-surface analysis (Press and Wilson, 1978). Two groups, each characterized by a set of multiple variables, can be discriminated by solving a set of simultaneous equations almost identical to those involved in multiple regressions. First, we defined the process of discrimination and carefully distinguish it from the related process of classification. As discussed earlier for fifty seven samples, microthermometric analysis were carried out on the double-polished wafers. A number of variables have been measured and calculated on each sample, including the homogenization temperature, salinity, pressure, elevation of sample, density of hydrothermal fluid and Cu grade. As shown in Fig. 11, it is not possible to separate the two alterations just with the given data by one variable. This can be graphically shown for two dimensional cases, as in Fig. 10, which is a scatter plot of the two groups of data. Although the two clusters of points overlap, it is apparent that a line of division could be placed between the two clusters such that most of the group 1 samples would be on one side and most group 2 samples would be on the other.

The problem is to find the linear combination of these variables that produces the maximum difference between the two previously defined alterations. If we find a function that produces a significant difference, we can use it to allocate new sample of fluid inclusion of unknown origin to one of the two original groups. In other words, new samples, not containing index mineral, can then be categorized as potassic or phyllic on the basis of the linear discriminant function of their thermometrical parameters (Potter *et al*., 1963).

A simple linear discriminant function transforms an original set of measurements on a sample into a single discriminant score. That score, or transformed variable, represents the specimen's position along a line defined by the linear discriminant function. If we regard present two groups as forming clusters of points in multivariate space, we must search for the one orientation along which the two clusters have the greatest separation while each cluster simultaneously has the least inflation.

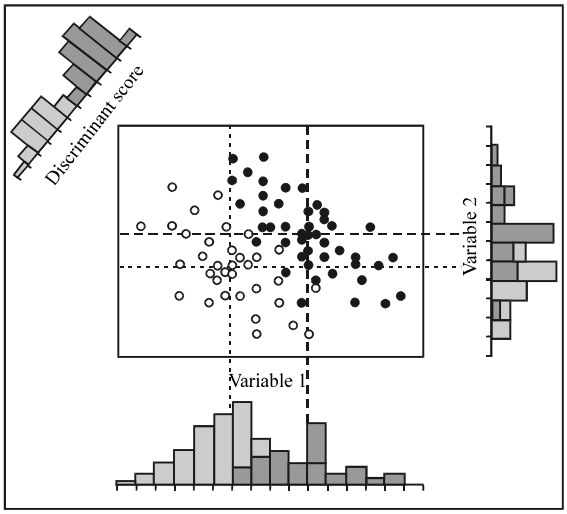

Fig. 10: Schematic plot of distributions of two variables with scatter plot of both variables. Samples indicated by open circles are belong group 1, those indicated by solid dots are belong group 2. Dashed lines indicate bivariate means of the two groups. Distribution of discriminant scores also is shown along line parallel to discriminant axis (Davis, 2002)

In matrix notation,

$$S\lambda = D \tag{1}$$

where, S is a 6×6 matrix of pooled variances and covariances of the 6 variables. λ (column vector) are used to represent the coefficients of the discriminant function. D, the column vector of 6 differences between the means of the 2 groups, which we will refer to as A (Potassic alteration) and B (Phyllic alteration). This equation can be solved by inversion and multiplication, as:

$$\lambda = S^{-1} D \tag{2}$$

where, S^{-1} is the inverse of the variance-covariance matrix formed by pooling the matrices of the sums of squares and cross products of the two alterations, A and B. To compute the discriminant function, we determined the various entries in the matrix equation. The mean differences are found by:

$$d_j = \overline{A_j} - \overline{B_j} = \frac{\sum_{i=1}^{n_a} a_{ij}}{n_a} - \frac{\sum_{i=1}^{n_b} b_{ij}}{n_b} \tag{3}$$

where, a_{ij} is the ith observation on variable j in alteration A and A_j is the mean of variable j in alteration A, which is

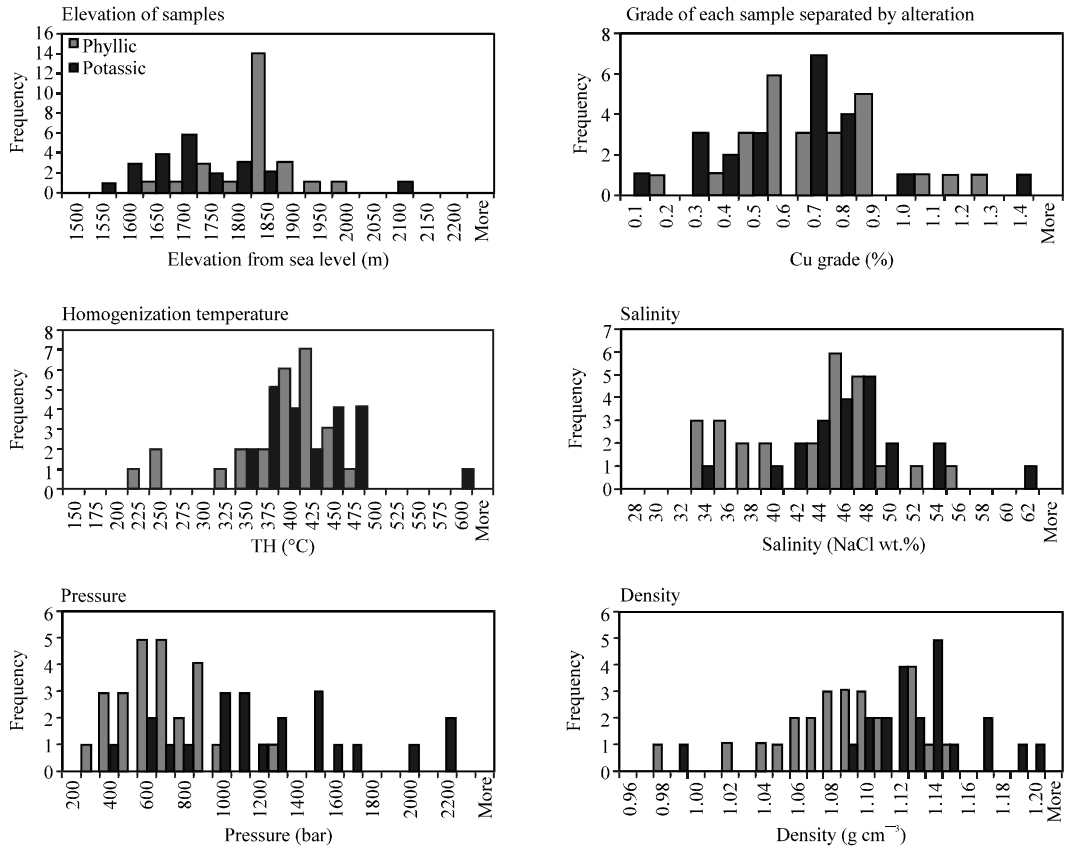

Fig. 11: Histogram of elevation, Cu grade, homogenization temperature, salinity, pressure and density for 47 analyzed and calculated point based on F.I. data shows that there is not a sharp boundary between the two potassic and phyllic alterations and they seems like two overlapped populations

the arithmetic average of the 22 observations of variable j in alteration A. The same conventions apply to alteration B. The difference between these multivariate means therefore also forms a vector:

$$D = \overline{A} - \overline{B} \tag{4}$$

In expanded form,

$$\begin{bmatrix} d_1 \\ d_2 \\ \dots \\ d_m \end{bmatrix} = \begin{bmatrix} \overline{A}_1 \\ \overline{A}_2 \\ \dots \\ \overline{A}_m \end{bmatrix} - \begin{bmatrix} \overline{B}_1 \\ \overline{B}_2 \\ \dots \\ \overline{B}_m \end{bmatrix} = \begin{bmatrix} 1695 \\ 0.57 \\ 413.6 \\ 46.3 \\ 1195 \\ 1.1243 \end{bmatrix} - \begin{bmatrix} 1811 \\ 0.68 \\ 375.9 \\ 42.5 \\ 623 \\ 1.0833 \end{bmatrix} = \begin{bmatrix} -116 \\ -0.11 \\ 37.7 \\ 3.8 \\ 572 \\ 0.041 \end{bmatrix}$$

To construct the matrix of pooled variances and covariances, a matrix of sums of squares and cross products of all variables is computed in alteration A and a similar matrix for alteration B.

$$SP_{Ajk} = \sum_{i=1}^{n_a} a_{ij} a_{ik} - \frac{\sum_{i=1}^{n_a} a_{ij} \sum_{i=1}^{n_a} a_{ik}}{n_a} \tag{5a}$$

where, a_{ij} denotes the ith observation of variable j in alteration A and a_{ik} denotes the ith observation of variable k in the same alteration. This quantity is the sum of squares of variable k whenever j = k. Similarly, a matrix of sums of squares and cross products is found for alteration B:

$$SP_{Bjk} = \sum_{i=1}^{n_b} b_{ij} b_{ik} - \frac{\sum_{i=1}^{n_b} b_{ij} \sum_{i=1}^{n_b} b_{ik}}{n_b} \tag{5b}$$

The sums of products matrix is denoted from alteration A as S_A and that from alteration B as S_B. The matrix of pooled variance can be found as:

$$S = \frac{S_A + S_B}{n_a + n_b - 2} \tag{6}$$

All of the entries necessary to estimate the discriminant function coefficients include:

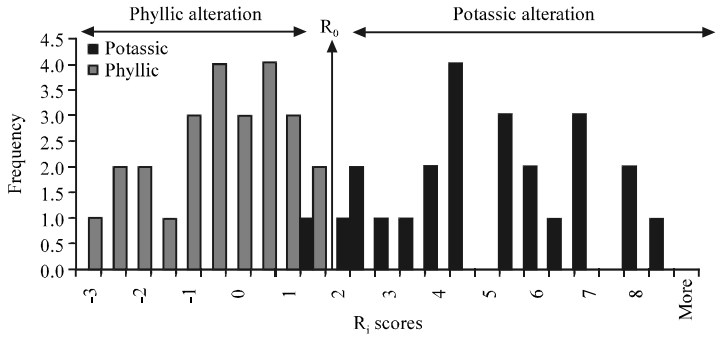

Fig. 12: Potassic and phyllic alteration projections of onto discriminant function line; R_0 is discriminant index

$$\underset{S^{-1}}{\begin{bmatrix} 0.00011254 & -0.0013571 & 1.80E\text{-}05 & -0.00024254 & -5.35E\text{-}07 & 0.019592 \\ -0.0013571 & 16.02 & 0.012493 & 0.017421 & -0.00044212 & 28.055 \\ 1.80E\text{-}05 & 0.012493 & 0.0012215 & -0.0089438 & -6.45E\text{-}05 & 0.98305 \\ -0.00024254 & 0.017421 & -0.0089438 & 0.10206 & 0.00025415 & -7.1033 \\ -5.35E\text{-}07 & -0.00044212 & -6.45E\text{-}05 & 0.00025415 & 1.38E\text{-}05 & -0.09043 \\ 0.019592 & 28.055 & 0.98305 & -7.1033 & -0.090426 & 1586 \end{bmatrix}} \times \underset{D}{\begin{bmatrix} -116 \\ -.11 \\ 37.7 \\ 3.8 \\ 572 \\ .041 \end{bmatrix}} = \underset{\lambda}{\begin{bmatrix} -.0126 \\ -.1702 \\ .0120 \\ -.069 \\ .0028 \\ 18.01 \end{bmatrix}}$$

The set of λ coefficients is found are entries in the discriminant function equation which has the form:

$$\begin{aligned} R_i &= \lambda_1 x_{1i} + \ldots + \lambda_6 x_{6i} \\ &= -0.0126 \times \text{elevation} - 0.1702 \times \text{Cu} + 0.012 \times T_h - 0.069 \\ &\times \text{Salinity} + 0.0028 \times \text{Pressure} + 18.012 \times \text{density} \end{aligned} \quad (7)$$

Equation 7 is a linear function; that is, all the terms are added together to yield a single number, the discriminant score, R_i. Substitution of the midpoint between the two group means into the discriminant function equation yields the discriminant index, R_0. That is, for each value of X_{ji} in Eq. 2, we insert the terms $x_j = (\bar{A}_j + \bar{B}_j)/2$ so we have,

$$\begin{aligned} R_0 &= (1753 \times -0.0126) + (.628 \times -0.17) + (395 \times 0.012) + \\ &(44.4 \times -0.069) + (909 \times 0.0028) + (1.104 \times 18.012) = 1.83 \end{aligned}$$

The discriminant index, R_0, is the point along the discriminant function line that is exactly halfway between the center of potassic alteration and the center of phyllic alteration. The R_0 is plotted as in Fig. 12. In fact, every observation in the analysis is entered into the equation and its position along the discriminant function located. Note that one member of alteration potassic is located on the phyllic alteration side of R_0 and one member of alteration phyllic is located on the potassic alteration side.

TESTS OF SIGNIFICANCE

The first step in a test of the significance of a discriminant function is to measure the separation or distinctness of the two alterations (Davis, 2002). This can be done by computing the distance between the centroids, or multivariate means, of the groups. Equation 8 used to find the standardized squared distance:

$$D^2 = D' S^{-1} D \quad (8)$$

This standardized measure of difference between the means of two multivariate groups is called Mahalanobis' distance. Substituting quantities into Eq. 8, we could obtain exactly the same distance measure by substituting the vector of mean differences into the discriminant function equation itself:

$$D^2 = \begin{bmatrix} -116 & -0.11 & 37.7 & 3.8 & 572 & 0.041 \end{bmatrix} \begin{bmatrix} & S^{-1} & \end{bmatrix} \begin{bmatrix} -116 \\ -0.11 \\ 37.7 \\ 3.8 \\ 572 \\ 0.041 \end{bmatrix} = 4.02$$

Mahalanobis' distance is visualized on Fig. 12, where, it is equal to the distance between $R_{A(potassic)}$ and $R_{B(phyllic)}$, we called it potassic-phyllic zone or transition. The significance of Mahalanobis' distance is tested using an F-test. The test of multivariate equality, using this more familiar statistic, is:

$$q = \left(\frac{n_a + n_b - m - 1}{(n_a + n_b - 2)m}\right)\left(\frac{n_a n_b}{n_a + n_b}\right) D^2 = \left(\frac{22 + 25 - 6 - 1}{(22 + 25 - 2)6}\right)\left(\frac{22 \times 25}{22 + 25}\right) 4.02 = 6.97 \quad (9)$$

$$F_{\alpha;m;n_1+n_2-m-1} = F_{0.015;6;40} = 5.75 \quad (10)$$

with m and (n_a+n_b-m-1) degrees of freedom.

Since the calculated q is grater than $F_{\alpha;m;n_1+n_2-m-1}$ in significance level of 0.015 and the freedom degree of 6 and 40 ($F_{0.15;6;40}$), so it is acceptable to chose all the variables for achieving a discriminant function which could be suitable when the equality of two alteration hypothesis is refused. So, it could be realized that the separation of two alteration based on the defined discriminant function could be done more precise.

DISCUSSION

The comparison of raw coefficient of λ for defining the share and effect of each variable in alteration separation is not useful. For example by ranking the λ, Cu grade has great part in separation, but as it is shown in Fig. 8, alteration separation based on Cu grade is impossible since the two populations are mixed together and Cu grade cannot be helpful in this matter. So, the Cu grade should locate in the last rank.

$$|\lambda_{Density}| > |\lambda_{Cu}| > |\lambda_{Salinity}| > |\lambda_{Elevation}| > |\lambda_{Th}| > |\lambda_{Pressure}|$$

So, a new variable named C is defined, which is multiplier of λ into the average of the same variable (M). So, the virtual value of λ which was changed during inversion of S matrix will remove and we can define the correct ranks of variables in alteration separation.

$$C_{Elevation} = \lambda_{Elevation} \times M_{Elevation} = -0.0126 \times 1756.86 = -22.23$$
$$C_{Cu} = \lambda_{Cu} \times M_{Cu} = -0.1702 \times 0.63 = -0.107$$
$$C_{Th} = \lambda_{Th} \times M_{Th} = 0.0120 \times 393.54 = 4.73$$
$$C_{Salinity} = \lambda_{Salinity} \times M_{Salinity} = -0.069 \times 44.24 = -3.05$$
$$C_{Pressure} = \lambda_{Pressure} \times M_{Pressure} = 0.0028 \times 890.68 = 2.50$$
$$C_{Density} = \lambda_{Density} \times M_{Density} = 18.0120 \times 1.1038 = 19.88$$

$$|C_{Elevation}| > |C_{Density}| > |C_{Th}| > |C_{Salinity}| > |C_{Pressure}| > |C_{Cu}|$$

By ranking the C, it seems that the elevation of samples has the most effect on alteration and then the density is located. The least effect is for Cu grade as it is expected. Against expectation, the difference between homogenization temperature and salinity of samples gained from the two alterations is not significance to separate the different alterations clearly.

CONCLUSIONS

The results show that the average of Th, Salinity, Pressure and density of fluids in quartz veinlets of potassic alteration are more than ones in phyllically altered samples. In potassic alteration zone, the average of homogenization temperature is 414°C while in phyllic alteration that is 376°C. As it is expected in potassic alteration the temperature of hydrothermal fluid is higher than that in phyllic zone, but there is not high difference between them. The salinity of the hydrothermal fluid has a high coherency with homogenization temperature, so the average amount of salinity in potassic samples is 46.3 (wt.% NaCl) which is a little bit higher than that of the phyllic samples (42.5 wt.% NaCl). As discussed above, the analysis were done on the three-phase fluid inclusions and as expected, this type of fluid inclusion shows high salinity in both alterations. Based on the location of potassic alteration, it is expected that the lithostatic pressure is much more than the phyllic one. It is realized that the average pressure in the potassic alteration is about 1195 bar while the average pressure in phyllic is about 623 bar). The density depends on the amount of the salinity of hydrothermal fluids, so the average density of the samples in potassic alteration is 1.124 (g cm^{-3}) which is higher than that in phyllic zone (1.083 g cm^{-3}). The average of Cu content in phyllic samples is higher that in the potassic ones and finally the average of elevation level of phyllic samples is much higher than that in the potassic samples. This result confirms that a geometric model could help to separate these alterations. As pointed out in the text, fluid inclusion micro-thermometric data and two auxiliary variables alone does not permit separation of potassic versus phyllic alteration fluid types.

This research has tried to discriminate the alterations using discriminant analysis method, a multivariate statistical method, based on different parameters. The discriminant analysis method decreases the multi-dimensional space including several parameters into a one-dimension, in a way the maximum separation could be observed in this axis. So, utilizing this method decreased the six-dimension space including Z, copper grade, density, pressure, salinity and Th into one dimension and yielded a single number, the discriminant score (R_i) that can do the most separation and also the alteration type and its intensity can be quantified.

This method gives us a specified limit R_0 value as the separation boundary. It is expected that the values larger

than R_0 belong to the potassic alteration and less than R_0 belong to the phyllic alteration. According to R_0 some of the potassic zone samples are in the phyllic zone and one of the phyllic zone samples is in the potassic zone region.

Through applying a discriminant analysis method beside the R_i, a set of λ coefficients is found. To improve the results, λ converted to an unbiased parameter entitled C, which is scalar product of λ and M (average of each variable). By ranking C, the effect of variables in alteration separation will be found. Elevation of sample is the most important variable. It means that the sample elevation plays an important role to separate the alteration zones. Density is the next important variable. We can assume the density of hydrothermal fluids as a function of combined homogenization temperature and salinity (based on the fluid inclusion studies). Rank of Cu grade could play the less effected role on the copper content within the alteration zones.

By using this function we can allocate the new fluid inclusions with unknown alteration to one of the two original alteration of potassic or phyllic. In other words, new samples not containing index minerals could then be categorized as potassic, phyllic or potassic-phyllic on the basis of the linear discriminant function of their variables.

REFERENCES

Brown, P.E., 1989. FLINCOR: A microcomputer program for the reduction and investigation of fluid inclusion data. Am. Mineral., 73: 1390-1393.

Brown, P.E. and W.M. Lamb, 1989. P-V-T properties of fluids in the system H_2O+CO_2+NaCl: New graphical presentations and implications for fluid inclusion studies. Geochimica et Cosmochim Acta, 53: 1209-1221.

Calagari, A.A., 2004. Fluid inclusion studies in quartz veinlets in the porphyry copper deposit at Sungun, East-Azarbaidjan, Iran. J. Asian Earth Sci., 23: 179-189.

Davis, J.C., 2002. Statistics and Data Analysis in Geology. 3rd Edn., John Wiley and Sons Publ., USA., ISBN: 978-0-471-17275-8, pp: 638.

Heinrich, C.A., 2005. The physical and chemical evolution of low-salinity magmatic fluids at the porphyry to epithermal transition: A thermodynamic study. Mineralium Deposita, 39: 864-889.

Hezarkhani, A. and A.E. Williams-Jones, 1998. Controls of alteration and mineralization in the Sungun porphyry copper deposit, Iran: Evidence from fluid inclusions and stable isotopes. Econ. Geol., 93: 651-670.

Hezarkhani, A., A.E. Williams-Jones and C.H. Gammons, 1999. Solubility and chalcopyrite deposition in the Sungun porphyry copper deposit, Iran. Miner. Deposita, 34: 770-783.

Heinrich, C.A., T. Pettke, W.E. Halter, M. Aigner-Torres and A. Audetat *et al*., 2003. Quantitative multi-element analysis of minerals, fluid and melt inclusions by laser-ablation inductively-coupled-plasma mass-spectrometry. Geochim Cosmochim Acta, 67: 3473-3497.

Hezarkhani, A., 2006a. Alteration/mineralization and controls of chalcopyrite dissolution/deposition in the raigan porphyry System bam-Kerman, Iran. Int. Geol. Rev., 48: 561-572.

Hezarkhani, A., 2006b. Petrology of intrusive rocks within the sungun porphyry copper deposit, Azarbaijan, Iran. J. Asian Earth Sci., 73: 326-340.

Kehayov, R., K. Bogdanov, L. Fanger, A. Von Quadt, T. Pettke and C.A. Heinrich, 2003. The Fluid Chemical Evolution of the Elatiste Porphyry Cu-Au-Pge Deposit, Bulgaria. In: Mineral Exploration and Sustainable Development, Eliopoulos, D.G. (Ed.). Millpress. Rotterdam, ISBN: 90-5966-015-3, pp: 1173-1176.

McLachlan, G.J., 1992. Discriminant Analysis and Statistical Pattern Recognition. 1st Edn., John Wiley, New York, ISBN: 9780471615316.

Meinert, L.D., J.W. Hedenquist, H. Sato and Y. Matsuhisa, 2003. Formation of anhydrous and hydrous skarn in Cu-Au ore deposits by magmatic fluid. Econ. Geol., 98: 147-156.

Potter, P.E., N.F. Shimp and J. Witters, 1963. Trace elements in marine and fresh-water argillaceous sediments. Geochim. Cosmochim. Acta, 27: 669-694.

Press, S.J. and S Wilson, 1978. Choosing between logistic regression and discriminant analysis. J. Am. Stat. Assoc., 73: 699-705.

Rapien, M.H., R.J. Bodnar, S.F. Simmons, C. Szabo and S.R. Sutton, 2003. The Embryonic Porphyry Copper System at White Island. 1st Edn., The Geochemical Society, New Zealand, ISBN: 1-887483-90-X.

Redmond, P.B., M.T. Einaudi, E.E. Inan, M.R. Landtwing, C.A. Heinrich, 2004. Copper deposition by fluid cooling in intrusion centered systems: New insights from the bingham porphyry ore deposit, Utah. Geology, 32: 217-220.

Shahabpour, J. and M. Doorandish, 2007. Mine drainage water from the sar cheshmeh porphyry copper mine, Kerman, IR Iran. Environ. Monit. Assess., 141: 105-120.

Shepherd, T., A.H. Rankin and D.H.M. Alderton, 1985. A Practical Guide to Fluid Inclusion Studies. 1st Edn., Blackie, London, ISBN-10: 041200601 4, pp: 239.

Sillitoe, R.H. and J.W. Hedenquist, 2003. Linkages Between Volcanotectonic Settings, Ore-Fluid Compositions and Epithermal Precious Metal Deposits. In: Volcanic, Geothermal and Ore-Forming Fluids: Rulers and Witnesses of Processes within the Earth. Simmons, S.F. and I. Graham (Eds.). Economics Geology Special Publication, ISBN: 978-3-540-27946-4, pp: 389-392.

Sillitoe, R.H., 1997. Characteristics and controls of the largest porphyry copper–gold and epithermal gold deposits in the circum- Pacific region. Aust. J. Earth Sci., 44: 373-388.

Sterner, S.M., D.L. Hall and R.J. Bodnar, 1988. Synthetic fluid inclusions. V. solubility of the system NaCl-KCl-H_2O under vapor-saturated conditions. Geochim. Cosmochim. Act., 52: 989-1005.

Stocklin, J.O. and J. Stocklin, 1977. Structural correlation of the alpine ranges between Iran and Central Asia. Memoire Hors Serie, No. 8 de la Soc. Geol. de France, 8: 333-353.

Tabachnick, B.G. and L.S. Fidell, 2000. Using Multivariate Statistics. 4th Edn., Allyn and Bacon, ISBN-10: 0321056779, pp: 966.

Watanabe, Y. and J.W. Hedenquist, 2001. Mineralogical and stable isotope zonation at the surface over the el salvador porphyry cu deposit, Chile. Econ. Geol., 96: 1775-1797.